N-Type Complimentary Semiconducting Polymer

Blends

William W. McNutt † , Aristide Gumyusenge † , Luke A. Galuska § , Zhiyuan Qian § , Jiazhi He † , Xiaodan Gu § , Jianguo Mei $^{\dagger \ddagger *}$

[†]Department of Chemistry and [‡]Birck Nanotechnology Center, Purdue University, West Lafayette, Indiana 47907, United States

§School of Polymer Science and Engineering, The University of Southern Mississippi, Hattiesburg, MS 39406, USA

Keywords: melt processing, semiconducting polymers, backbone engineering, organic field effect transistors, n-type, polymer blends

ABSTRACT: Complimentary semiconducting polymer blends (c-SPBs) have been demonstrated as an effective approach to balance performance and processing of semiconducting polymers for organic field-effect transistors. All previously reported c-SPBs have been exclusively based on p-type polymers. In this report, we designed and synthesized naphthalene diimide (NDI) based matrix polymers and systematically studied n-type charge transport behaviors of their corresponding polymer blends. NDI- C_m (m = 3-7) polymers displayed low melting points (55-105 °C) allowing for the lowest temperature melt-processing of organic transistors to date with

mobilities up to $1.01*10^{-3}$ cm²V⁻¹s⁻¹. NDI-C_m polymers were revealed to be nearly amorphous by GIXRD and thinfilm UV-Vis which explain the lowered thermal transitions and observed poor charge transport. Utilizing c-SPB with 5% fully conjugated P(NDI2OD-T2), the transistor performance improved up to 100-fold of the pure matrix polymer despite the low crystallinity of NDI-C_m thinfilms.

INTRODUCTION

Semiconducting polymers have gained attention because of their wide application potential in solar cells, light-emitting diodes, transistors, and other devices. 1-3 Organic semiconducting polymers are conceivably more mechanically conformable and lightweight than their inorganic counterparts and can be fabricated from solutions with fast printing techniques such as ink-jet printing and slot-die coating. 4-5 Organic semiconductors are held together by secondary forces (van der Waals force), and the weak intermolecular interactions render these polymers to have poor charge transport characteristics. 6 The focus in the field has mainly been to improve the electrical performance of conjugated polymers which initially was significantly lower than inorganic materials. The performance of semiconducting polymers has steadily increased over time and is now comparable and superior to amorphous silicon. Unfortunately, most of the early developed high-performance semiconducting polymers are only soluble and processed from toxic chlorinated solvents. 8 Sometimes, it even requires processing them under high temperatures. 9 Thus, it virtually makes them incompatible with environmental standards and industrial manufacturing processes. There are a variety of efforts to improve the processability of semiconducting polymers, ranging from molecular design (i.e., side chain engineering and precursor method) to process engineering (i.e., the formation of nanoparticles). 10-12 Our group previously focused on a completely different

approach, and introduced the concept of complimentary semiconducting polymer blends (c-SPBs). 13-20 c-SPBs are composed of a semiconducting matrix polymer with conjugation-break spacers along the polymer backbone and a fully conjugated polymer that functions as a tie chain. 13 With the conjugation break spacers, matrix polymers expectedly present inadequate electrical properties, but greatly improve their desired physical properties such as solubility and melt temperature.¹⁷ The blending of the matrix polymer with 1-5% fully conjugated analogue (tiechain) nearly brings the hole mobility back to that of fully conjugated polymer. Further, the lowered melting transition of the blends allowed our group to prepare melt-processed OFETs, eliminating the use of chlorinated solvents. 18 Up to date, donor-acceptor type polymers containing conjugation break spacers and their corresponding complimentary blends have been exclusively demonstrated with p-type charge transport. It is not clear if this blending design strategy can be successfully extended to n-type donor-acceptor type polymers. Facchetti and Yao et al. reported matrix poly[N,N'-bis(2-octyldodecyl)-1,4,5,8the only-known polymer n-type naphthalenedicarboximide-2,6-diyl]-alt-5,5'-[2,2'-(1,2-ethanyl)bithiophene] (P(NDI2OD-TET) where a saturated -CH₂-CH₂- group is inserted in between the two thienyl units to break polymer backbone π -conjugation.²¹ They studied this polymer and their fully conjugated analog poly[N,N'bis(2-octyldodecyl)-1,4,5,8-naphthalenedicarboximide-2,6-diyl]-alt-5,5'-(2,2'-bithiophene) (P(NDI2OD-T2)) and found that the spacer had a profound impact on the redox properties and cycling stability in the context of energy storage. In other words, the concept of n-type c-SPBs has not been validated there. Considering the difference between p-type and n-type charge transport, it thus provides ample motivation to investigate and validate n-type c-SPBs performance.

In this study, we prepared five naphthalene diimide (NDI) based matrix polymers (NDI- C_m , m = 3-7) where a conjugation break spacer (CBS) of three to seven methylene groups is inserted into

P(NDI2OD-T2). The influence of conjugation break spacer length on physical, optical, and electrical properties has been fully explored with these NDI-C_m polymers. Further, we studied the blends of NDI-C_m and P(NDI2OD-T2) and their electronic properties in OFETs. The obtained results proved that the concept of n-type c-SPBs is valid. Built on this discovery and taking advantage of the low melt transitions of the blends, melt-processed OFETs with n-type c-SPBs were fabricated. The blend containing 5 wt% of P(NDI2OD-T2) in NDI-C3 offered averaged electron mobilities up to 0.012 cm²V⁻¹ s⁻¹. The melt processing temperature of 100°C represented the lowest temperature to obtain melt-processed semiconducting thin films to date. Additionally, thin film morphologies have been probed with atomic force microscopy (AFM) and grazing incidence x-ray diffraction (GIXRD).

RESULTS AND DISCUSSION

Scheme 1. Synthetic Routes for the Monomers and Polymers (NDI- C_m , m = 3-7)

$$\begin{array}{c} 1.) \ nBuLi \\ 2.) \ Br(CH_{2})_m Br \\ \hline THF, -78^{\circ}C \\ (m = 3 \text{ to } 7) \\ \hline \\ C_{8}H_{17} \\ \hline \\ O \\ O \\ Br \\ \hline \\ O \\ O \\ O \\ \hline \\ Br \\ \hline \\ O \\ O \\ \hline \\ O \\ O \\ \hline \\ O \\ \\ O \\ \\ O \\ \hline \\ O \\ \\ O \\ \\ O \\ \hline \\ O \\ \\$$

Monomer and Polymer Synthesis. Synthetic routes for the NDI-C_m polymers are shown in Scheme 1. The synthesis for the linear methylene CBS monomers were performed as previously reported.¹⁷ Polymers were prepared by Stille coupling polymerization; experimental details can be found in the supporting information/experimental section. The obtained polymers were purified by successive Soxhlet extraction with acetone, hexane, and chloroform. The chloroform/hexane fraction was collected and precipitated in methanol. The solid was collected by vacuum filtration and dried under vacuum at elevated temperatures for shorter spacers (3/4); longer spacers (5-7) were dried only under vacuum due low melting points. With increasing CBS length, the solubility of the NDI-C_m polymers noticeably increased, longer spacers (5-7) showed great solubility in hexane even with comparable molecular weights as the shorter spacers containing polymers. The polymers were characterized by ¹H NMR, gel permeation chromatography (GPC), thermal gravimetric analysis (TGA), differential scanning calorimetry (DSC), UV-Vis spectroscopy (UVvis), and cyclic voltammetry (CV). The results of the characterizations can be found in Table 1. Molecular weight and polydispersities (PDI) were estimated by GPC with tetrahydrofuran (THF) as the eluent at 40°C. The molecular weights range from 12.6 to 50.8 kDa with PDI between 1.4 and 3.4. Due to insolubility in THF, the molecular weight and PDI of P(NDI2OD-T2) was estimated by GPC with 1,2,4-trichlorobenzene (TCB) as the eluent at 160°C and found to be 157.5 kDA with a PDI of 2.0. ¹H NMRs of the five matrix polymers gave very sharp peaks, unlike the broad peaks typically observed polymer systems. This suggests the polymers are completely unaggregated in chloroform solutions.

Table 1. Physical Properties of the NDI-Cm and P(NDI2OD-T2) Polymers

Polymer	Mn(kDa)/PDI ^a	$T_d(^{\circ}C)^b$	T _m (°C) ^c	λ_{max}^{abs} (nm)		E_a^{opt}	Energy Levels (eV)	
				Soln.d	Thinfilme	(eV)f	$E_{\rm HOMO}^{\rm g}$	$E_{\rm LUMO}^{\rm h}$
NDI-C3	50.8/1.6	436	104 / 60	519	520	2.08	-5.82	-3.74
NDI-C4	21.7/1.9	436	105 / 76	520	517	2.08	-5.86	-3.78

NDI-C5	12.6/1.4	428	71 / 54	520	518	2.08	-5.86	-3.77
NDI-C6	18.0/1.3	425	55	520	518	2.08	-5.86	-3.78
NDI-C7	28.6/2.0	425	48	521	520	2.08	-5.86	-3.78
P(NDI2OD-T2)	157.5/2.0 ⁱ	448	312	701	705	1.55	-6.22	-4.69

a)Tetrahydrofuran (THF) as the eluent at 40 °C. b)Decomposition Temperature . c)Melting Temperature. d)Chloroform Solution e)Dropcast films on glass substrates, annealed at 50 °C. f)Calculated from the onset absorption $E_g^{opt} = 1240/\lambda$ onset abs (nm). g) Calculated using the equation $E_{Homo} = E_{Lumo} - E_g^{opt}$ LUMO energy level determined by CV $E_{Lumo} = -[4.8 + (E_{red} - E_{1/2(ferrocene)})]$ eV. i) 1,2,4-trichlorobenzene (TCB) as eluent at 160 °C.

Polymer Characterizations. Optical properties of the synthesized matrix polymers were evaluated by UV-Vis spectroscopy and corresponding results are summarized in Table 1. Solution and solid-state spectra are shown in Figure 1. In chloroform solutions all polymers exhibited a high energy transition peak close to 400 nm and a lower energy peak maximum absorption at 520 nm which is attributed to the well-defined chromophore on the polymer backbone. This is in contrast with P(NDI2OD-T2) that shows significant red-shift due extended conjugation length. Pure matrix thinfilms show similar absorbance with no bathochromic shift from π -aggregation as is typically expected from conjugation polymer thin films like that observed in P(NDI2OD-T2) thinfilm. This implies that NDI-C_m polymers are a disordered system. This is in good agreement with GIXRD results shown in Table S1. Energy levels of the matrix polymers were investigated using cyclic voltammetry (CV; Figure 1). All NDI-C_m polymers have two reversible reduction peaks. The first peak is at -0.7 V providing a low lying LUMO level at -3.7 eV. The HOMO levels estimated from $E_{\text{lumo}} - E_{\text{g}}^{\text{opt}}$ (Table 1) were found to be -5.82-5.86 eV for all matrix polymers. Thermal stability of the polymers was studied by thermal gravimetric analysis (TGA) and the results are summarized in Table 1 and Figure S3. All polymers showed good thermal stability with no decomposition until around 425°C. Phase transitions were studied by differential scanning calorimetry (DSC) and the results are summarized in Table 1 and Figure 1D;

thermograms are shown in Figure S4. Thermal characterization of NDI-C_m polymers by DSC proved difficult due to the apparent long recrystallization times. The melting points of the polymers were not always observable on the 2nd DSC scans which is typically reported to ensure no influence of thermal history. Melting transitions are observed in the range of 48-102 °C. The melting point decreases with increasing CBS length. NDI-C_m polymers have drastically lowered melting points in comparison with fully conjugated P(NDI2OD-T2). All melting points observed are highly favorable for melted processing at low temperatures.

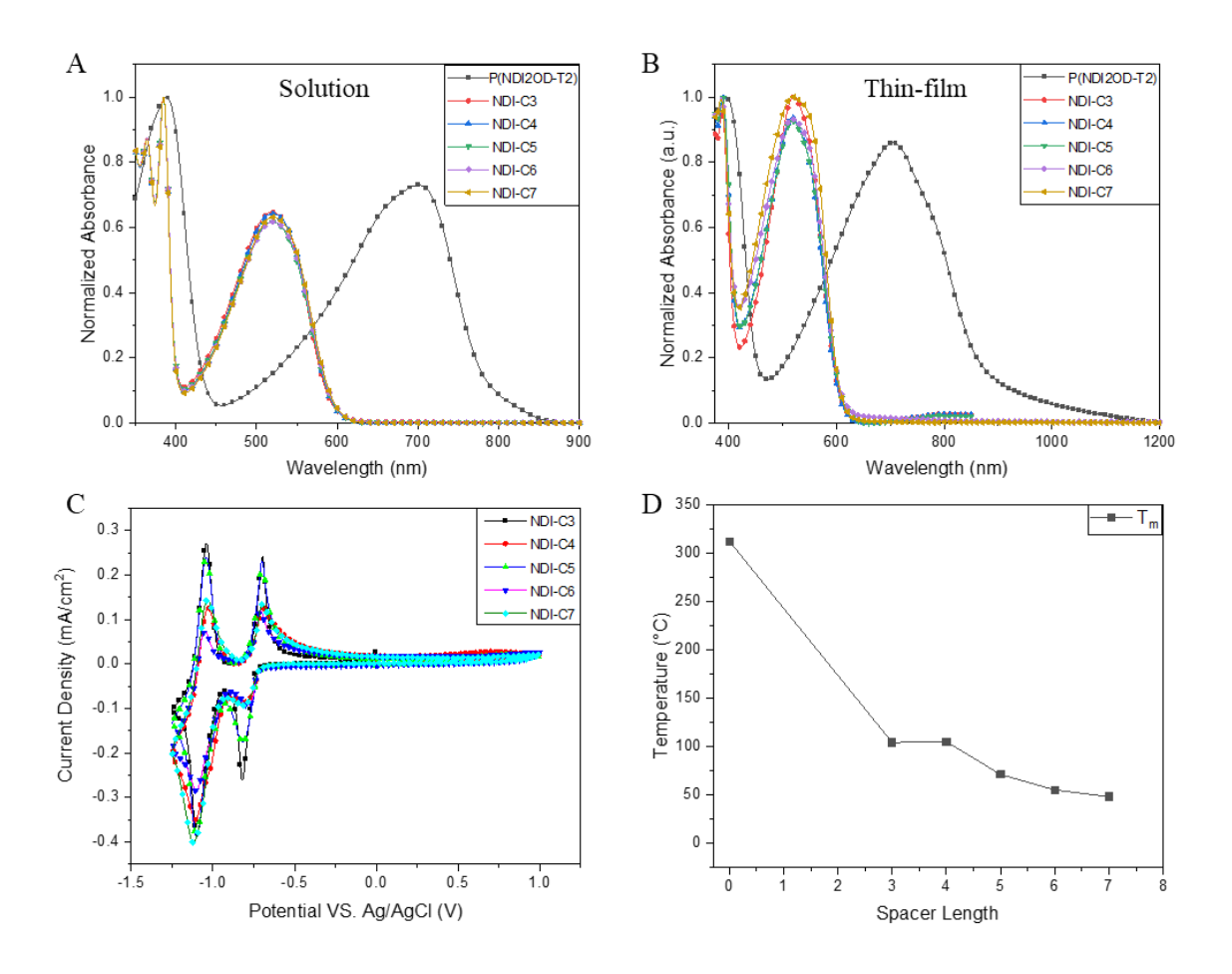


Figure 1. UV-Vis Spectra of NDI-C_m and P(NDI2OD-T2) Polymers, (A) Chloroform Solutions. (B) Thinfilms. (C) Cyclic Voltammetry of NDI-C_m polymers, CV and DPV of P(NDI2OD-T2) in SI. (D) Melting Point Trend of NDI-C_m and P(NDI2OD-T2) Polymers, DSC thermograms in Figure S4.

Charge Transport Properties of Matrix Polymers and Polymer Blends. The charge transport properties of NDI- C_m (m = 3-7) and their c-SPBs with the tie chain polymer P(NDI2OD-T2) were investigated using bottom-gate, bottom contact field-effect transistor devices. Pure matrix polymer thinfilms were prepared by melt processing as previously reported apart from lower processing temperature at 100° C. ¹⁴ For c-SPB thin films, the matrix polymers and 5% tie-chain were premixed in solution and the dried mixed pellets were used to fabricate the transistor devices. Average mobilities were extracted from 20 different devices for all the studied polymers.

Table 2. Charge Transport Characteristics of P(NDI2OD-T2), NDI-C_m and c-SPB with 5% of Tie Chain Polymer P(NDI2OD-T2) Annealed at 100°C

Polymer	Pure Polymers	5% c-SPB			
	$\mu_{eavg} cm^2 V^{-1} s^{-1}$	$\mu_{emax} cm^2 V^{-1} s^{-1}$	$V_{th}(V)$	$I_{\rm on}/I_{\rm off}$	$\mu_{emax} cm^2 V^{-1} s^{-1}$
NDI-C3	4.02*10 ⁻⁴	1.01*10 ⁻³	+23.6	1.02*10 ³	0.012
NDI-C4	5.13*10 ⁻⁵	2.01*10 ⁻⁴	+20.1	3.19*10 ³	8.90*10 ⁻³
NDI-C5	1.10*10 ⁻⁵	1.3*10 ⁻⁵	+22.1	2.34*10 ³	1.03*10 ⁻³
NDI-C6	<1.0*10 ⁻⁶	<10*10 ⁻⁶	NA	NA	5.53*10 ⁻⁵
NDI-C7	<1.0*10 ⁻⁶	<10*10 ⁻⁶	NA	NA	6.30*10 ⁻⁵
P(NDI2OD-T2)	0.098	0.178	+24.0	$2.84*10^2$	-

For all matrix polymers only n-type transport was observed in contrast to P(NDI2OD-T2) which demonstrates an ambipolar behavior (Figures S10, S13). The measured electron mobility from the matrix polymers was strongly diminished with insertion of conjugation break spacers and continued to rapidly decrease with length. Only shorter spacer length (3-5) demonstrated measurable mobility while with longer spacer lengths of 6/7, the mobility was near the limit of detection. This was in good agreement with the previously reported DPP system. The low mobilities were also in good agreement with the low crystallinity and weak π - π aggregation displayed by the matrix polymers in GIXRD and UV-Vis respectively, as well as the high lying

LUMO level shown by CV. The extracted OFETs results are summarized in Table 2 and representative characteristic transfer curves are shown in Figure S10. It should be noted that these devices were tested in air for comparison with the parent tie-chain despite the inherent sensitivity of n-type materials towards oxygen and moisture. It was thus encouraging that even with methylene units inserted to break the backbone conjugation, these matrix polymers could still exhibit extractable charge mobilities. Unlike previously reported DPP-C_m polymers, NDI-C_m polymers display no odd-even effect trend in mobility.¹⁷

With these matrix polymers in hand, we investigate complimentary semiconducting polymer blends, an approach that has been demonstrated by our research group as a robust strategy to enhance charge-transport properties of semiconducting matrix polymers. ^{13-14, 16-19} This method has yet to be demonstrated with n-type materials. To test the validity of c-SPBs for n-type matrix polymers, we blended 5 wt% of the fully conjugated P(NDI2OD-T2) (tie-chain) parent polymer with the matrix polymer. This led to an improvement of up to 100-fold for n-type charge transport for NDI-C5. In the case of NDI-C3 5% blend, a record high electron mobility amongst n-type, melt-processed polymers, 0.012 cm²V⁻¹ s⁻¹, could be obtained from the melt processed blend films. When the conjugation break spacer length was further increased, the blending efficiency could only boost the charge mobilities to moderate values as shown in Table 2. This could be partly due to the lack of crystallinity in the matrix polymer as, c-SPBs rely on the tie chain polymer interconnecting the crystalline domains to achieve effective charge mobility. Since the increase in the spacer length shows to lower the matrix' crystallinity, we would expect the blending effect to start declining. Further increase in the P(NDI2OD-T2) content of the blends showed to only moderately increase the mobility (Figure S13) as predicted from the complimentary blending design that charge mobility will begin to plateau (Figure 2).¹³

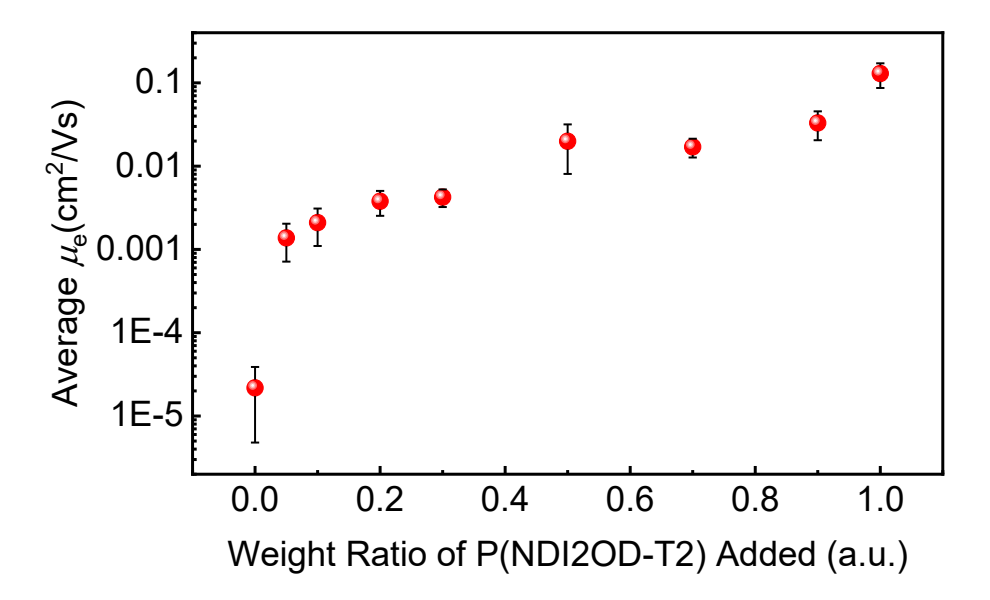


Figure 2. N-type mobility trend for NDI-C5 c-SPBs with increasing P(NDI2OD-T2) content.

Morphology and Molecular Packing Information. Thinfilm morphology characterizations and molecular packing studies were carried out to probe the charge transporting pathways in the fabricated OFETs devices. Atomic force microscopy (AFM) was used to characterize solid-state morphologies, and grazing incidence x-ray diffraction (GIXRD) for the molecular packing in thin films. AFM images (Figure S5) revealed smooth surface morphology for all the NDI-C_m polymers. These morphologies came to support the shiny metallic luster observed at the micro-scale from the melt-pressed films (Figure 3c). This smoothness showed to increase when the films were treated to temperatures higher than of the corresponding melting points. The smoothness of all thinfilms allows for easy delamination from the substrate into free-standing thinfilms. All thinfilms could easily be transferred and laminated onto prepatterned substrates for OFETs fabrication. This lack of any large surface aggregates in thin films could also support the non-aggregation seen in the UV-Vis spectra. In contrast, pure spin cast thinfilms of the rigid fully conjugated tie-polymer P(NDI2OD-T2) showed large aggregates (Figure 3), in accordance to its red-shifted UV-Vis

maximum absorption. No notable morphological changes were observed when treated at the same temperatures as the matrices. The tie-polymer did not show signs of melting until 300 °C in accordance to the DSC results. For c-SPBs, a significant morphology change could be observed when only 5% of the tie-chain polymer were used. In comparison to pure NDI-C5, for instance, the thinfilms showed to became much rougher indicative of solid-state aggregates formation (Figure 3). Increasing the content of the tie-chain P(NDI2OD-T2) lead to gradually rougher surface film morphologies (Figure S6) which could support the gradual increase in corresponding mobilities. The thinfilms surfaces do not show signs of phase segregation like previously reported systems.

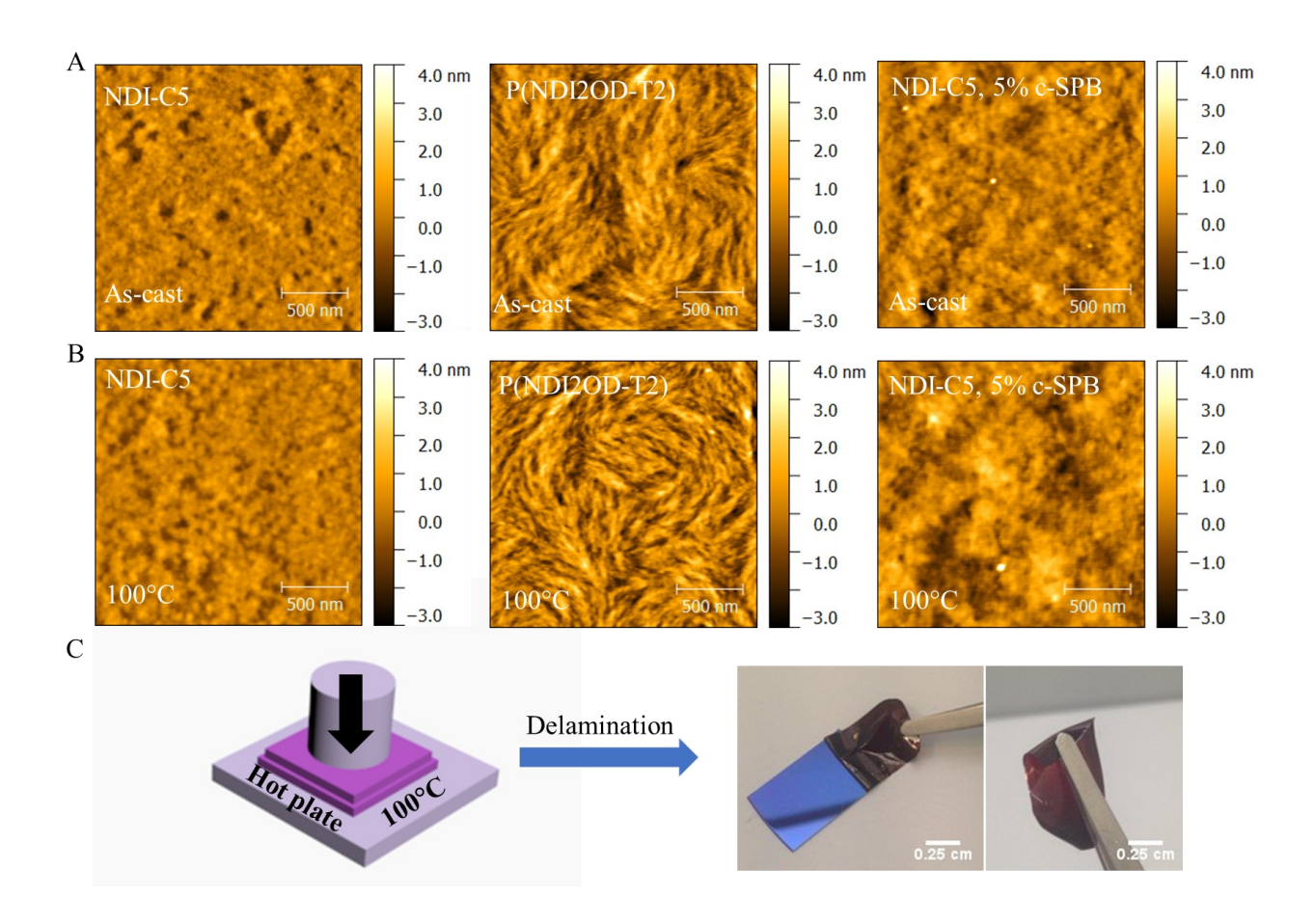


Figure 3. (A) AFM images of NDI-C5, P(NDI2OD-T2), NDI-C5 5% c-SPB thinfilms as cast. (B) Same thinfilms after annealing at 100 °C to show NDI-C5 and 5% c-SPB melted into a

smoother film for delamination. (C) Technique demonstration of melt-processing bulk polymer material into thinfilms and subsequent delamination.

GIXRD results of the matrices revealed low crystallinity for the studied matrices in comparison to the fully conjugated analogue. Weak lamellar stacking could be observed in the out-of-plane directions for NDI-C_m thin films. No strong π - π stacking could be found for the matrices, and these results were not surprising due to low charge carrier mobilities observed. P(NDI2OD-T2) showed a clear predominantly face-on orientation with a strong π - π stacking signal in the out-of-plane signal. The contribution of this packing to the blends containing a small portion of P(NDI2OD-T2) was also evident, and a π - π stacking peak started to evolve in the blends. Figure S7/8 show the GIXRD 2D patterns of P(NDI2OD-T2), the matrix polymers, and the corresponding 5% c-SPBs. A careful extraction of the peak positions was carried out to probe the influence of spacer length on the packing behavior as well as the impact of the rigid tie chains on the blends. The extracted peak positions and intensities are summarized in Table S2 and the corresponding 1D linecuts can be found in the supporting information. A Gaussian fitting was performed to evaluate peak intensities. Despite the weakly diffracting nature of the blend films, the impact of having a small percentage of tie-chains within the blends showed to initiate the formation of charge-carrying aggregates within the predominantly amorphous matrices. This approach is thus sought after as a mean to enhance charge transport in n-type polymer systems.

CONCLUSION

In summary, we have prepared a set of 5 NDI-C_m (m = 3-7) matrix polymers containing conjugation break spacers from 3-7 methylene units. DSC revealed low melting points more suitable for melt-processing temperatures. The low melting point can be attributed to the lack of crystallinity and π -aggregation as revealed by GIXRD and UV-Vis measurements and ¹H NMR.

The first melt-processed n-type complimentary semiconducting polymer blends were demonstrated. Performance of NDI- C_m polymer transistors could be increased up to 100-fold by blending with 5% P(NDI2OD-T2) tie-chain polymer. c-SPBs continue to be an emerging method for tailoring both physical and electrical properties of organic thinfilm transistors. Mechanical properties are currently underway to characterize the apparent ductile nature of these new polymers.

EXPERIMENTAL DETAILS

Materials and Characterizations. All reagents and starting materials were purchased from Sigma-Aldrich and SunaTech and used without further purification unless otherwise noted. ¹H NMR spectra were recorded using Bruker ARX 400 at 293 K with deuterated chloroform as solvent. For NDI-C_m polymers room temperature gel permeation chromatography (GPC) was performed in tetrahydrofuran under room temperature with a Polymer Laboratories PL-GPC20. The molecular weights matrix polymers were calculated using a calibration curve based on polystyrene standards. An Agilent PL-GPC-220 system high temp (HT)-GPC was utilized to characterize the molecular weights of P(NDI2OD-T2) in this study. This system is equipped with 3 pLGel Olexis (13 µm particle size) in series in addition to a differential refractive index (RI) detector, a dual angle (15° and 90°) light scattering (LS) detector, and a viscometer (VS) detector. Prior to the GPC analysis, the polymers were dissolved by shaking in 1,2,4-trichlorobenzene (TCB) at a concentration of 1-2 mg/mL for 2 hrs at 160°C and subsequently filtered through a 2 μm stainless steel filter. All polymers were run in the instrument at 160°C using TCB as an eluent. The chromatograms were worked up from the RI signal utilizing a narrow standard polystyrene calibration (14 points, ranging from 162 g/mol to 3,242,000 g/mol). TGA measurements were carried out on a Mettler-Toledo TGA/DSC 3+ equipped with a Huber minichiller 300 under nitrogen gas purge rate of 50 mL/min. The samples were heated from 25 °C to 700 °C at a heating rate of 10 °C/min. A Mettler-Toledo DSC 3+ equipped with a FRS6+ sensor and a Huber TC100 intracooler was utilized for DSC measurements, under dry nitrogen gas purge with a flow rate of 50 mL/min. A heat-cool-heat cycle with rate of 30 °C/min was applied. UV-Vis-NIR spectra were recorded on a Cary 50 spectrophotometer (350–1200 nm). Atomic force microscopy images were obtained on a Veeco Dimension 3100 AFM in tapping mode. GIWAXS were performed at a sample to detector distance of ~ 300 mm under a helium environment with an incident beam energy of 12.7 keV and an incidence angle of 0.12°. The data was collected on beamline 11–3 at the Stanford Synchrotron Radiation Lightsource. The analysis was performed using Nika software package within Wavemetrics Igor, in combination with WAXS tools. The cyclic voltammetry (CV) experiments were performed in a three-electrode cell with a scan rate of 40 mV/s. The working electrode was the platinum bottom electrode coated with NDI polymers; the reference electrode was a leakless Ag/AgCl electrode; the counter electrode is the platinum wire and the electrolyte is 0.2 M TBAPF₆ in propylene carbonate.

Thinfilm formation and Device Characterization Methods. Material P(NDI2OD-T2) (3.3 mg/mL) and NDI- C_m (10 mg/mL) were dissolved in chloroform at 50 °C stirred overnight. The c-SPB solution were obtained by mixing the X wt% of P(NDI2OD-T2) solutions into (100–X) wt% NDI- C_m solutions. Before use, the P(NDI2OD-T2) solution was stirred and heated up to 50 °C. The c-SPB solid was dried from its solutions.

OFET device Fabrication. A heavily n-doped Si wafer with a 300 nm SiO₂ surface layer (capacitance of 11 nF/cm²) was employed as the substrate with Si wafer serving as the gate electrode and SiO₂ as the dielectric. The gold S/D electrodes were sputtered and patterned by photolithography technique. For the vapor-based octadecyltrichlorosilane (OTS) modification, the

silicon wafer (with Au bottom contacts) were first cleaned with (H_2SO_4 (98%): H_2O_2 (30% water solution) = 7:3) for 20 minutes. It was then washed with deionized (DI) water several times, and further subjected to sonication sequentially in DI water and acetone for 6 min each. After drying inside an oven, the silicon wafer was then put into a clean petri dish with a small drop of OTS. The dish was then covered and heated in a vacuum oven at 120 °C for 3 hours, resulting in the formation of an OTS self-assembled monolayer on the surface. The OTS modified substrates were rinsed successively with hexane, ethanol, and chloroform, and dried by nitrogen. The semiconductor layer was deposited on the OTS-treated Si/SiO₂ substrates by spin coating with spin speed of 1500 rpm. and spin time of 120 s. The devices were then annealed in nitrogen glovebox. For P(NDI2OD-T2) and c-SPB OFETs, the channel length was 60 μ m and channel width was 1000 μ m. For NDI-C_m, the channel length was 5 μ m and channel width was 1000 μ m.

Melt-processed thin film fabrication. Solution-based OTS-modification was used to prepare the substrates for melt processing. The NDI- C_m and c-SPB materials are sticky to glass or bare silicon wafer and hard to peel-off, thus the OTS-modification is essential for peel-off process. For film fabrication, the NDI- C_m or c-SPB materials was put between to OTS-modified substrates on a hot plate. After the materials get melted, a heavy object (~ 4 kg) was put on top of the substrates to press the materials. With different press time and temperatures, different film thickness can be achieved. For peel-off process, the two substrates were first separated. The film was then peeled off, starting from the corner or the edge of the substrate.

Electrical characterization. Device characterization was carried out using Keithley 4200 in ambient air for all devices. For hot-pressed c-SPB OFETs, the electrical measurement was carried out at room temperature in ambient air. The field-effect mobility was calculated in the saturation regime by using the equation $I_{DS} = (\mu W C_i/2L)(V_G - V_T)^2$, where I_{DS} is the drain–source current,

μ is the field-effect mobility, W is the channel width, L is the channel length, C_i is the capacitance

per unit area of the gate dielectric layer, V_G is the gate voltage, and V_T is the threshold voltage.

Three batches of devices and more than 5 devices in each batch were tested, and their results were

in good agreement.

ASSOCIATED CONTENT

Supporting Information

Characterization details and additional experimental data are in Supporting Information. This

material is available free of charge *via* the Internet at http://pubs.acs.org.

AUTHOR INFORMATION

Corresponding Author

*Email: jgmei@purdue.edu (J.M.).

ORCID

Jianguo Mei: 0000-0002-5743-2715

Notes

The authors declare no competing financial interest.

Funding

This work was supported by the NSF CAREER Award (NSF DMR/Polymer, #1653909).

ACKNOWLEDGMENTS

Part of this work performed by Z.Q.; L. G., and X. G. was supported by NSF Office of Integrative

Activities #1757220. L.G. was partially supported by National Science Foundation Division of

Graduate Education (DGE) #1449999. The Authors would also like to thank Alexander Ayzner

16

group for performing the initial GIXRD measurements. W.M. and J.M. are grateful for the financial support from National Science Foundation Polymer Program (#1653909).

REFERENCES

- 1. Dimitrakopoulos, C. D.; Malenfant, P. R. L., Organic Thin Film Transistors for Large Area Electronics. Advanced Materials 2002, 14 (2), 99-117.
- 2. Forrest, S. R., The path to ubiquitous and low-cost organic electronic appliances on plastic. Nature 2004, 428 (6986), 911-918.
- 3. Facchetti, A., π-Conjugated Polymers for Organic Electronics and Photovoltaic Cell Applications. Chemistry of Materials 2011, 23 (3), 733-758.
- 4. Maunoury, J. C.; Howse, J. R.; Turner, M. L., Melt-Processing of Conjugated Liquid Crystals: A Simple Route to Fabricate OFETs. Advanced Materials 2007, 19 (6), 805-809.
- 5. Baklar, M. A.; Koch, F.; Kumar, A.; Domingo, E. B.; Campoy-Quiles, M.; Feldman, K.; Yu, L.; Wobkenberg, P.; Ball, J.; Wilson, R. M.; McCulloch, I.; Kreouzis, T.; Heeney, M.; Anthopoulos, T.; Smith, P.; Stingelin, N., Solid-State Processing of Organic Semiconductors. Advanced Materials 2010, 22 (35), 3942-3947.
- 6. Quinn, J. T. E.; Zhu, J.; Li, X.; Wang, J.; Li, Y., Recent progress in the development of n-type organic semiconductors for organic field effect transistors. Journal of Materials Chemistry C 2017, 5 (34), 8654-8681.
- 7. Sirringhaus, H., 25th Anniversary Article: Organic Field-Effect Transistors: The Path Beyond Amorphous Silicon. Advanced Materials 2014, 26 (9), 1319-1335.
- 8. Brandão, L.; Viana, J.; Bucknall, D. G.; Bernardo, G., Solventless processing of conjugated polymers—A review. Synthetic Metals 2014, 197, 23-33.
- 9. Sui, Y.; Deng, Y.; Du, T.; Shi, Y.; Geng, Y., Design strategies of n-type conjugated polymers for organic thin-film transistors. Materials Chemistry Frontiers 2019, 3 (10), 1932-1951.
- 10. Mei, J.; Bao, Z., Side Chain Engineering in Solution-Processable Conjugated Polymers. Chemistry of Materials 2014, 26 (1), 604-615.
- 11. Uemura, T.; Mamada, M.; Kumaki, D.; Tokito, S., Synthesis of Semiconducting Polymers through Soluble Precursor Polymers with Thermally Removable Groups and Their Application to Organic Transistors. ACS Macro Letters 2013, 2 (9), 830-833.
- 12. Wu, J.; You, L.; Lan, L.; Lee, H. J.; Chaudhry, S. T.; Li, R.; Cheng, J.-X.; Mei, J., Semiconducting Polymer Nanoparticles for Centimeters-Deep Photoacoustic Imaging in the Second Near-Infrared Window. Advanced Materials 2017, 29 (41), 1703403.
- 13. Zhao, Y.; Zhao, X.; Roders, M.; Qu, G.; Diao, Y.; Ayzner, A. L.; Mei, J., Complementary Semiconducting Polymer Blends for Efficient Charge Transport. Chemistry of Materials 2015, 27 (20), 7164-7170.
- 14. Gumyusenge, A.; Zhao, X.; Zhao, Y.; Mei, J., Attaining Melt Processing of Complementary Semiconducting Polymer Blends at 130 °C via Side-Chain Engineering. ACS Applied Materials & Interfaces 2018, 10 (5), 4904-4909.
- 15. Xue, G.; Zhao, Y.; Zhao, X.; Li, H.; Mei, J., Zone-Annealing-Assisted Solvent-Free Processing of Complementary Semiconducting Polymer Blends for Organic Field-Effect Transistors. Advanced Electronic Materials 2018, 4 (1), 1700414.

- 16. Zhao, X.; Xue, G.; Qu, G.; Singhania, V.; Zhao, Y.; Butrouna, K.; Gumyusenge, A.; Diao, Y.; Graham, K. R.; Li, H.; Mei, J., Complementary Semiconducting Polymer Blends: Influence of Side Chains of Matrix Polymers. Macromolecules 2017, 50 (16), 6202-6209.
- 17. Zhao, X.; Zhao, Y.; Ge, Q.; Butrouna, K.; Diao, Y.; Graham, K. R.; Mei, J., Complementary Semiconducting Polymer Blends: The Influence of Conjugation-Break Spacer Length in Matrix Polymers. Macromolecules 2016, 49 (7), 2601-2608.
- 18. Zhao, Y.; Zhao, X.; Roders, M.; Gumyusenge, A.; Ayzner, A. L.; Mei, J., Melt-Processing of Complementary Semiconducting Polymer Blends for High Performance Organic Transistors. Advanced Materials 2017, 29 (6), 1605056.
- 19. Zhao, Y.; Zhao, X.; Zang, Y.; Di, C.-a.; Diao, Y.; Mei, J., Conjugation-Break Spacers in Semiconducting Polymers: Impact on Polymer Processability and Charge Transport Properties. Macromolecules 2015, 48 (7), 2048-2053.
- 20. Zhao, Y.; Gumyusenge, A.; He, J.; Qu, G.; McNutt, W. W.; Long, Y.; Zhang, H.; Huang, L.; Diao, Y.; Mei, J., Continuous Melt-Drawing of Highly Aligned Flexible and Stretchable Semiconducting Microfibers for Organic Electronics. Advanced Functional Materials 2018, 28 (4), 1705584.
- 21. Liang, Y.; Chen, Z.; Jing, Y.; Rong, Y.; Facchetti, A.; Yao, Y., Heavily n-Dopable π -Conjugated Redox Polymers with Ultrafast Energy Storage Capability. Journal of the American Chemical Society 2015, 137 (15), 4956-4959.

TOC

